Journal of Materials Science and Engineering B 5 (5-6) (2015) 248-253
doi: 10.17265/2161-6221/2015.5-6.007

Evolution of the Pore Size Distribution in Nanoporous Alumina Membranes with Anodization Voltage in Oxalic Acid

Mesbah Elyaagoubi[1], Youssef Najih[1], Mohyeddine. Khadiri[2], Amane. Oueriagli[2], Abdelkader Outzourhitb[2] and Mustapha Mabrouki[1*]

1. Industrial Engineering Laboratory, Faculty of Science and Technology,Sultan My SlimaneUniversity, BeniMellal 23010, Morocco

2. Solid State Physics and Thin FilmsLaboratory, Faculty of Science Semlalia, Cadi Ayyad University,Marrakech 40400, Morocco

Abstract: The effect of voltage on nanopores formed via electrochemical anodization of high purity Aluminum was investigated. The electrochemical bath consisted of a 0.3 M oxalic acid electrolyte. A platinum electrode was used as the counter-electrode, and an aluminum sheet as the anode. The anodization process was carried out at a temperature of 7 °C at various voltages ranging from 30 to 55V. It was observed that during the anodizing process, both the current density and the nanopore size increase as the applied voltage increases. The morphology and the distribution of nanopores were analyzed by SEM (Scanning electron microscope). It was found that mean pore diameter increased from 43 to 100 nm as the voltage is increased from 30 to 55 V. the polydispersity of the pore size was found to be minimum at 40 V.

Keywords: Aluminum sheet, electrochemical anodization, nanopores, pore size distribution.

1. Introduction

Nanoporous anodic aluminum oxide membranes have attracted considerable attention due to their multiple potential uses. These membranes offer nanochannels of high regularity and a high diameter-to-length aspect ratios through their thicknesses [1, 2]. Numerous synthetic techniques were used to prepare highly ordered nanostructured matrices such as e-beam lithography [3], nanoimprint lithography [4], soft lithography [5], NSL (Nanosphere lithography) [6], MBE (Molecular beam epitaxy) [7], laser ablation [8], sol-gel method [9], and various template methods [10-14], electrochemical anodization [15].

The electrochemical method using two-step anodization for the fabrication of nanoporous aluminum oxide with regular structure in oxalic acid was first reported by H. Masuda in 1995 [16]. The pore formation is affected by several parameters, such as the anodization voltage, the concentrationand the nature of acid solutions, the electrolyte temperature and the first anodization time. It was reported that sulphuric acid solution is suitable for the formation of smaller pores with diameter between 10 and 30 nm [17-19]; whereas oxalic acid solution is used for the formations of medium size pores (~30-100 nm) [16, 20-22].

The porous anodic alumina membranes were used for fabrication of various nanomateriels, such as polymeric nanowires, metallic nanowires [23], 3D nanodots [24], metallic nanotubes [25]. Other applications of these nanoporous membranes such as gas separation [26], drug delivery [27], solar cells [28] and membrane in solid acid fuel cells [29] were also been reported.

In all of these studies, it was observed that the growth rate of the pore is highly correlated with the concentration and nature of acid solutions and the

*Corresponding author: Mustapha Mabrouki, PhD., professor, research fields: materials sciences and physics. E-mail: Mus_mabrouki@yahoo.com.

anodic voltage. The aim of this work is to study the effect of the anodic voltages, on the fabrication of highly ordered pore arrays in aluminum thin sheets in oxalic acid.

2. Materials and Methods

The samples (aluminum sheets of 2 mm in thickness) were ultrasonically cleaned in acetone, rinsed with deionized water and then annealed at 400 °C for 3 h in vacuum to reduce mechanical stress in these substrates. They were subsequently electropoliched in a mixture of perchloric acid and ethanol (1:4 v/v $HClO_4$: C_2H_5OH) at constant voltage of 15 V for approximately 3 min at room temperature. The cleaned aluminum sheets were then used as the anode and Pt foil as the cathode in the anodization cell. The first anodization was carried out in 0.3 M oxalic acid at a temperature of 7 °C and a fixed voltage of 40 V. After the first anodization, the sample was dipped in a mixture solution (0.4 M H_3PO_4 + 0.2 M H_2CrO_4) at 60 °C for 5 h to remove the formed porous film. The second anodization was then carried at various voltages 30, 40 and 55 V at 7 °C in 0.3 M oxalic acid. The pores were then enlarged using a 5% H_3PO_4 at 30.0 °C for 30 min. The first and second anodization lasted respectively 3 h and 8 h.

The Current-Time curves of the 2nd anodizing at different voltages were recorded by a computer -controlled ammeter. These curves were used to monitor the anodization process as well as to analyze the growth mechanism.

The morphology of the formed membranes was observed by a scanning electron microscope (SEM JEOL JSM5500). The imageJ software [30] was used for estimation of the interpore spacing, pore-size distribution and mean pore diameter. FFT (Fast Fourier transforms) of SEM (Scanning electron microscope) images were calculated by using the scanning probe image processor Image J.

3. Results and Discussion

Fig. 1 shows the SEM images of the surface of the porous anodic alumina membranes anodized at a temperature, 7 °C and for three different voltages 30, 40 and 55 V in 0.3 M oxalic acid solution.

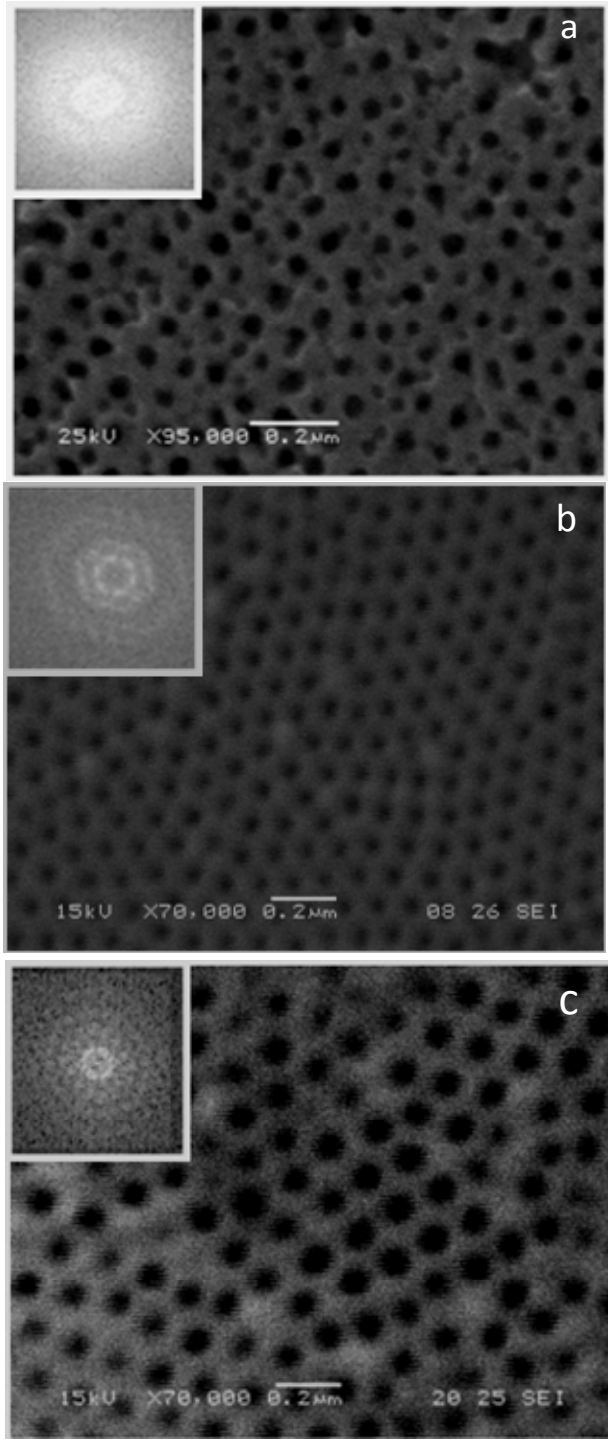

Fig. 1 SEM images of the top surface of nanoporous alumina prepared by two-step anodizing in 0.3 Moxalic acid at 7 °C. The inset in (a)-(c) corresponding tothe FFT images at different voltages: (a) 30 V, (b) 40 V and (c) 55 V.

As shown in Fig. 1a for an anodization of 30 V, the pores are randomly distributed and their size is not uniform. For an anodization voltage of 40 V (Fig. 1b) the pores are regularly distributed in a honey-comb array which is in agreement with the results reported in the literature [16-22]. At a high voltage of 55 V, the pore size distribution is not perfectly uniform, and the average pore size increased (Fig. 1c). These trends can be clearly seen in the FFT of these images shown in the upper part of Fig. 1. The FFT of the images corresponding to an anodization voltage of 30 V show a halo-type structure which is typical of randomly distributed pores (or structures). For samples anodized at 40 V, a hexagonal arrangement can be clearly seen in the FFT of the images (Fig. 1b). At 55 V anodization voltages, the hexagonal distribution starts to be degraded Fig. 1c. This qualitative arrangement analysis made by FFT shows the anodizing 40 V leads to the best pores organization.

The SEM photograph in Fig. 2 shows the cross-section of the porous anodic alumina membranes. The pores are parallel to each other and perpendicular to the surface of the membrane.

The pore size distributions, depicted in the histograms of Fig. 3, was evaluated from the measurement of the pore sizes in the three images. The distribution is rather sharp in the case of 40 V. In addition, the mean pore diameter increases as the anodization voltage. These trends can be clearly seen in table 1, where the mean pore sizes (xc), the standard deviation and the polydispersity ((σ/xc) × 100%) are given.

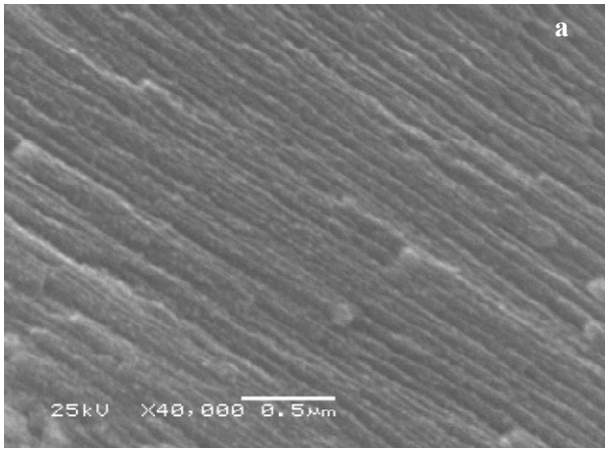

Fig. 2 Cross-sectional SEM images of nanoporous alumina prepared by two-step anodizing in 0.3 M oxalic acid at 7 °C and 40 V.

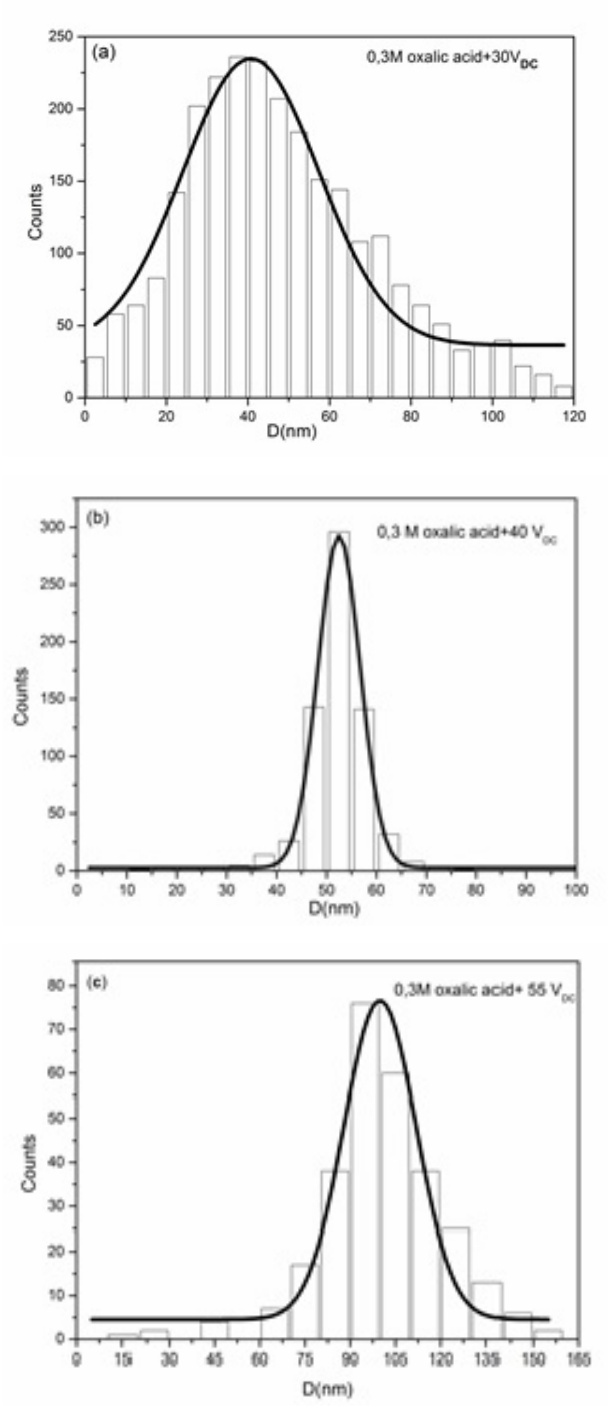

Fig. 3 Distribution histogram of the pore diameter for various anodizing potentials Anodizing of aluminum was conducted in 0.3 M oxalic acid at7 °C for three different anodization voltages: (a) 30, (b) 40 and (c) 55 V.

Table 1 Pore size of nanoporous alumina produced by two-step anodizing in 0.3 M oxalic acid at 30, 40 and 55 V at 7 °C.

	30 V	40 V	55 V
Average pore size xc (nm)	40.71	52.49	99.87
W (nm)	33.36	8.44	23.97
Standard deviation (σ) = W/2 (nm)	16.69	4.22	11.98
Average pore size with error = xc ± σ (nm)	40.71 ± 16.69	52.49 ± 4.22	99.87 ± 11.98
Polydispersity = (σ/xc) × 100%	41%	8%	12%

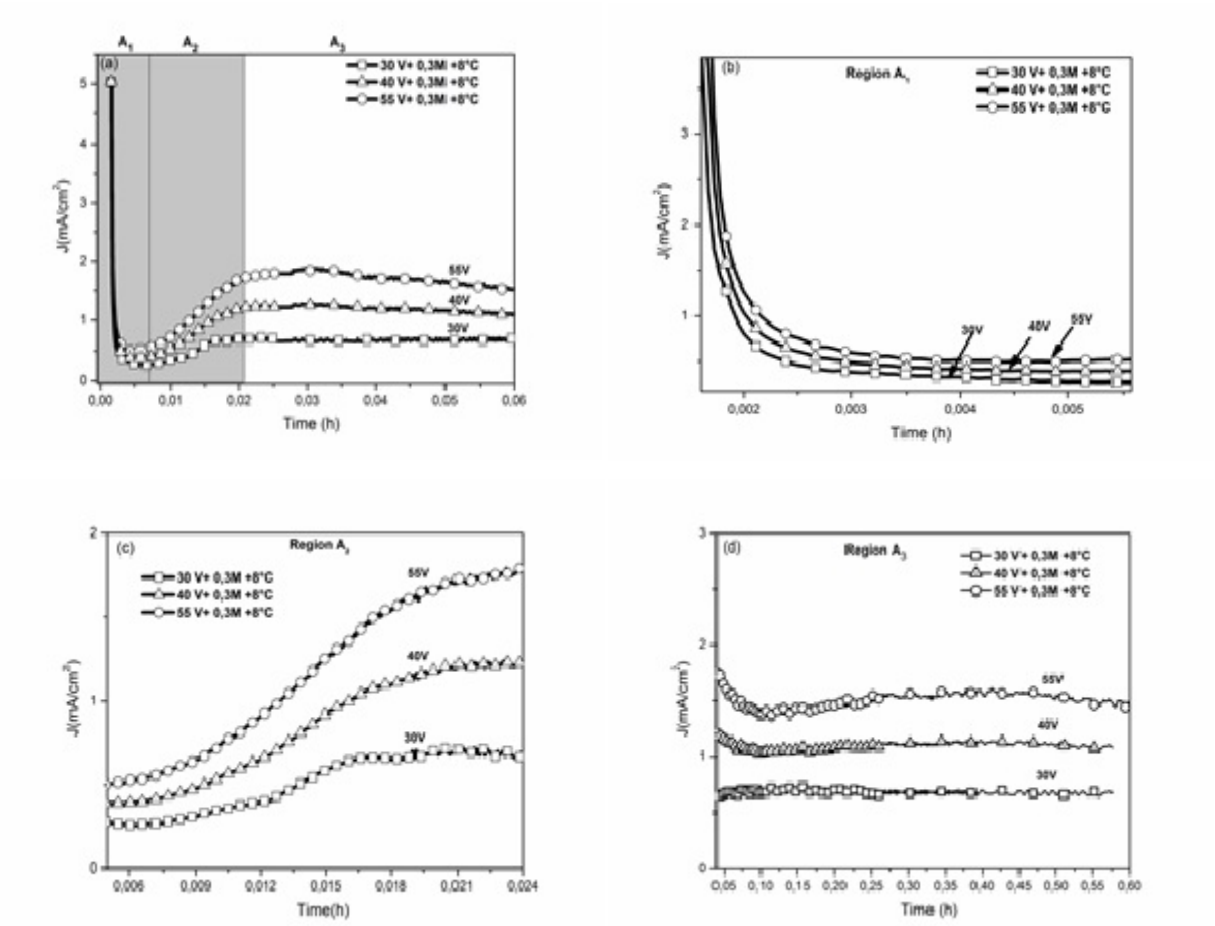

Fig. 4 (a) Current-time (I-t) curves of nanoporous alumina prepared by two-step anodizing in 0.3 M oxalic acid at7 °C for three different anodization voltages of 30, 40 and 55 V; (b) and (c) are I-t curves of region A1 and region A2 respectively; (d) I−t curves of region A_3.

For 30 V the polydispersity of this structure is 41% while the average pore size is 41 nm and the interpore distance is in the range of 74 nm. For 40 V, an average pore diameter of ~ 52 nm is obtained while the Polydispersity of this structure is 8% and the interpore distance is in the range of 100 nm. On the other hand, for samples anodized at 55 V the polydispersity of this structure increased to about 12%, while the average pore size is 100 nm and the interpore distance is in the range of 150 nm. These results show that the process of self-ordering nanopores in alumina occurs in a solution of oxalic acid at 40V.

Fig. 4 shows the current-time (I-t) curves measured for three different anodization voltages of 30, 40 and 55 V during the second anodization in oxalic acid. Three different regions (noted A1, A2 and A3) can be clearly distinguished in this figure. These regions are shown in more details in Fig. 4d. In region A1, there is

a sharp decrease in the current density for all the applied voltages as shown in Fig. 4b. It is well known that at this initial stage (region A1), an oxide barrier layer is formed on the aluminum surface. The surface oxidation takes place for a period of 5 to 10 s. The similarity of the I-t curves in this region is an indication that the oxide growth mechanism is similar at this initial stage of the anodization for the three anodization voltages.

In the region A2 (Fig. 4c), the shapes of the I-t curves are also similar for all voltages, except for the positions and the heights of the peaks. In the beginning of this region, there is an increase in the current density which indicates that the dissolution of the barrier layer is initiated. When the current density reaches the maximum, regular pores with a constant wall thickness are formed [31]. The differences in the position and the height of the peaks (Fig. 4c) can be explained by localized dissolution of Al_2O_3 at the oxide/electrolyte interface, which leads to the formation of vertical pores [32]. The increase in the current density for higher voltages suggest a higher dissolution rate compared to the oxide growth rate. In other words, the pore formation process is faster at greater anodizing voltages

In region A3 (Fig. 4d), the current density is rather constant during the anodization at 30 and 40 V while an oscillation is observed for 55 V (increase and then a decrease). Thus, for high anodization voltages, it is hard to form ordered pore arrangements due to the unstable current density as can be seen in Fig. 1c.

However, for the anodization voltage of 30 V, although the current density is very stable, disordered pore arrangements were obtained (Fig. 1a). The anodization voltage of 40 V is an optimum voltage since the current stable and the pores are well ordered (Fig. 1b).

4. Conclusion

Porous anodic alumina membranes were successfully fabricated at 7 °C in 0.3 M oxalic acid in a voltage range of 30 to 55 V using a two steps anodization. The different applied voltages were found to produce pores. The SEM results showed the effect of voltage on the arrangement of the pores and pore size. It was observed that during the anodizing process, the current density and the pore size increase as the applied voltage is increased. An anodization voltage of 40 V is the optimal voltage to obtain a perfectly hexagonal nanoporous structure during anodization of aluminum in 0.3 M oxalic acid at 7 °C.

References

[1] Shingubara, S. 2003. “Fabrication of Nanomaterials Using Porous Alumina Templates.” *Nanoparticle Research* 5: 17-30.

[2] Kim, J. H., Ahn, K. S., Lee, K. N., Kim, C. O. and Hong, J. P. 2004. “Size Control of Anodic Alumina Oxide Layer by an Anodic Oxidation Method for the Application of Magnetic Quantum Dots and Carbon Nanotubes.” *Korean Physical Society* 45 (1): 141-4.

[3] Ohkouchi, S., Nakamura,Y., Ikeda, N., Sugimoto, Y. and Asakawa, K. 2007. “Selective Growth of Ordered InGaAs Quantum Dots on Patterned Substrates with Nano-Hole Arrays.” *Journal of Crystal Growth* 744: 301-2.

[4] Chou, S. Y., Krauss, P. R., Zhang ,W., Guo, L., and Zhuang, L. 1997. “Sub-10 nm Imprint Lithography and Applications.” *Vacuum Science & Technology B* 15 (6): 2897-904.

[5] Yang, P., Deng, T., Zhao, D., Feng, P., Pine, D. and Chmelka, B. F. et al. 1998. “Hierarchically Ordered Oxides.” *Science* 282: 2244-6.

[6] Haynes, C. L. and Van Duyne, R. P. 2001. “Nanosphere Lithography: A Versatile Nanofabrication Tool for Studies of Size-Dependent Nanoparticle Optics.” *Physical Chemistry B* 105 (24): 5599-611.

[7] Schubert, L., Werner, P., Zakharov, N. D., Gerth, G., Kolb, F. M. and Long, L. et al. 2004. “Silicon Nanowhiskers Grown on 〈111〉 Si Substrates by Molecular-Beam Epitaxy.” *Applied Physics Letters* 84: 4968-70.

[8] Zavedeev, E. V., Petrovskaya, A. V., Simakin, A. V. and Shafeev, G. A. 2006. “Formation of Nanostructures upon Laser Ablation of Silver in Liquids.” *Quantum Electronics* 36 (10): 978-80.

[9] Jia, F. L., Zhang, L. Z., Shang, X. Y. and Yang ,Y. 2008. “Non-Aqueous Sol–Gel Approach towards the Controllable Synthesis of Nickel Nanospheres, Nanowires, and Nanoflowers.” *Advanced Materials* 20: 1050-4.

[10] Lazzari, M. and López-Quintela, M. A. 2003. “Block Copolymers as a Tool for Nanomaterial Fabrication.”

Advanced Materials 15 (19): 1583-94.

[11] Deng, Z. and Mao, C. 2003. "DNA-Templated Fabrication of 1D Parallel and 2D Crossed Metallic Nanowire Arrays." *Nano Letters* 3 (11): 1545-8.

[12] Walter, E. C., Zach, M. P., Favier, F., Murray, B. J., Inazu, K. and Hemminger, J. C. 2003. "Metal Nanowire Arrays by Electrodeposition." *ChemPhysChem* 4: 131-8.

[13] Hulteen, J. C., Menon, V. P. and Martin, C. R. 1996. "Template Preparation of Nanoelectrode Ensembles. Achieving the 'Pure-Radial' Electrochemical-Response Limiting Case." Chemical Society, Faraday Transactions 92: 4029-32.

[14] Wade, T. L. and Wegrowe, J. -E. 2005. "Template Synthesis of Nanomaterials." *European Physical Journal Applied Physics* 29: 3-22.

[15] Stępniowski, W. J. and Bojar, Z. 2011. "Synthesis of Anodic Aluminum Oxide (AAO) at Relatively High Temperatures. Study of the Influence of Anodization Conditions on the Alumina Structural Features. " *Surface and Coatings Technology* 206: 265-72.

[16] Masuda, H. and Fukuda, K. 1995. "Ordered Metal Nanohole Arrays Made by a Two-Step Replication of Honeycomb Structures of Anodic Alumina." *Science* 268: 1466-8.

[17] Jessensky, O., Muller, F. and Gösele, U. 1998. "Self-Organized Formation of Hexagonal Pore Arrays in Anodic Alumina." *Applied Physics Letters* 72 (10): 1173-5.

[18] Manzano, C. V., Martín, J. and Martín-Gonzalez, M. S. 2014. "Ultra-Narrow 12 nm Pore Diameter Self-Ordered Anodic ALumina Templates." *Microporous and Mesoporous Materials* 184: 177-83.

[19] Belwalkar, A., Grasing, E., Van Geertruyden, W., Huang, Z. and Misiolek, W. Z. 2008. "Effect of Processing Parameters on Pore Structure and Thickness of Anodic Aluminum Oxide (AAO) Tubular Membranes." *Journal of Membrane Science* 319: 192-8.

[20] Masuda, H., Hasegawa, F. and Ono, S. 1997. "Self-Ordering of Cell Arrangement of Anodic Porous Alumina Formed in Sulfuric Acid Solution." *Electrochemical Society* 144: 127-30.

[21] Zaraska, L., Stępniowski, W. J., Jaskuła, M. and Sulka, G. D. 2014. "Analysis of Nanopore Arrangement of Porous Alumina Layers Formed by Anodizing in Oxalic Acid at Relatively High Temperatures." *Applied Surface Science* 305: 650-7.

[22] Jeong, S. Y., An, M. C., Cho, Y. S., Kim, D. J., Paek, M. C. and Kang, K. Y. 2009. "Preparation of Anodic Aluminum Oxide Templates on Silicon Substrates for Growth of Ordered Nano-Dot Arrays." *Current Applied Physics* 9: 101-3.

[23] Das, B., Mandal, M., Mandal, K. and Sen, P. 2014. "Influence of Alumina Membrane on Magnetic Properties for Thermally Annealed CoPt Alloy Nanowires." *Colloids and Surfaces A: Physicochemical and Engineering Aspects* 443: 398-403.

[24] Imai, T. and Nomura, S. 2004. "Quantum Dot Arrays Prepared with Self-Organized Nanopore and its Photoluminescence Spectra." *Physica E: Low-dimensional Systems and Nanostructures* 21: 1093-7.

[25] Yue, S., Yan, Z., Shi,Y. and Ran, G. 2013. "Synthesis of Zinc Oxide Nanotubes within Ultrathin Anodic Aluminum Oxide Membrane by Sol-Gel Method." *Materials Letters* 98: 246-9.

[26] Gooding, J. J. 2005. "Nanostructuring Electrodes with Carbon Nanotubes: A Review on Electrochemistry and Applications for Sensing ." *Electrochimica Acta* 50: 3049-60.

[27] Gong, D., Yadavalli, V., Paulose, M., Pishko, M. and Grimes, C. A. 2003. "Controlled Molecular Release Using Nanoporous Alumina Capsules." *Biomedical Microdevices* 5 (246): 75-80.

[28] Darder, M., Aranda, P., Hernández-Vélez, M., Manova, E. and Ruiz-Hitzky, E. 2006 . "Encapsulation of Enzymes in Alumina Membranes of Controlled Pore Size. " *Thin Solid Films* 495: 321-6.

[29] Bocchetta, P., Ferraro, R. and Di Quarto, F. 2009. "Advances in Anodic Alumina Membranes Thin Film Fuel Cell: CsH_2PO_4 Pore-Filler as Proton Conductor at Room Temperature." *Power Sources* 187 :49-56.

[30] Image J National Institute of Mental Health, Bethesda, Maryland, USA. http:// 564 rsb.info.ni.gov/ij.

[31] Parkhutik, V. P. and Shershulsky, V. I. 1992. "Theoretical Modelling of Porous Oxide Growth on Aluminum." *Physics D: Applied Physics* 25: 1258-63.

[32] Ma, D., Li, S. and Liang, C. 2009. "Electropolishing of High-Purity Aluminium in Perchloric Acid and Ethanol Solutions." *Corrosion Science* 51:713-8.